International Symposium
On Turbulence and Shear Flow
Phenomena (TSFP-9)
June 30 - July 3, 2015 *Melbourne, Australia*



# INNER-OUTER INTERACTION PREDICTIVE MODEL FOR WALL-BOUNDED TURBULENCE SUBJECTED TO PRESSURE GRADIENT EFFECT

**Romain Mathis**
Laboratoire de Mécanique de Lille
CNRS UMR 8107, Université Lille Nord de France
59655 Villeneuve d'Ascq, France
romain.mathis@univ-lille1.fr

**I. Marusic, N. Hutchins & J. P. Monty**
Department of Mechanical Engineering
University of Melbourne
Victoria, 3010 Australia
imarusic@unimelb.edu.au

**Z. Harun**
Department of Mechanical and Materials Engineering
The National University of Malaysia 43600 Bangi, Malaysia
zambri@eng.ukm.my

## ABSTRACT

In an early work, Marusic, Mathis & Hutchins (2010) developed a model ables to reconstruct the streamwise turbulence fluctuation of the inner-layer in zero-pressure-gradient, flat-plate, turbulent boundary layer. The originality of this model, which is based on scales interaction, is that it requires as input only one localised information (*e.g.* one measurement point) about large-scale log-region events. The present study is dedicated to the model's assessment under pressure gradient effects. Results show the need to undertake the calibration when change in external conditions occurs, pointing out the non-universality of the model's parameters (Adrian, 2010). This preliminary work shows that the model is able to predict the streamwise velocity statistics of the inner-layer up to the second order.

## INTRODUCTION

Wall-bounded turbulent flows remain nowadays one of the main concern in industrial applications, as they are linked to drag loss, pressure drop, etc. Despite several decades of intense researches, the understanding and prediction of the near-wall turbulence remain limited and challenging. This founds its cause in the wide range of scales that develop and produce multiple complex interactions. This degree of complexity is measured by the Reynolds number, usually very (extremely) high in most of applications, and difficult to reproduce or simulate in laboratory. The discovery of the existence of recurrent features has shed light that despite an obvious disorder of the flow, some structures seem to be organised, eventually quantifiable and modelisable (Townsend, 1976; Cantwell, 1981). The numerous studies that have followed have shown the existence of a large and complex hierarchy of scales interacting together (Kim & Adrian, 1999; Adrian, 2007). Particularly, two distinct organisations have been identified. The near-wall cycle, apparently to small-scale motions organised in streamwise streaks, and large-scale log-region events such as hairpin (Adrian *et al.*, 2000), or superstructures (Hutchins & Marusic, 2007; Dennis & Nickels, 2011). Recently, it has been shown that the large-scale motions developing within the logarithmic region of the turbulent boundary layer, influence the near-wall field through superposition and modulation mechanisms (Hutchins & Marusic, 2007; Mathis *et al.*, 2009). The superposition mechanism is seen as a footprint of the large-scales onto the near-wall small-scale field (as a long-wavelength trend). The modulation mechanism is characterised by a locally change in the small-scale fluctuations magnitude depending on the sign of the large-scale log-region momentum: if it is negative the small-scale fluctuations are attenuated and *vice-versa*. Furthermore, the large-scale activity has been found to increase with increasing Reynolds number and is believed to be related, at least to a great extend, to the Reynolds number effects (Hutchins & Marusic, 2007).

Based on the above observations, Marusic and coworkers (Marusic *et al.*, 2010; Mathis *et al.*, 2011) have recently proposed a predictive model for zero-pressure-gradient (ZPG) smooth-wall turbulent boundary layer, which is able to reconstruct the near-wall streamwise fluctuating velocity field (say for $z^+ < 200$) based on a single point measurement taken in the log-layer away from the wall. Here, the fluctuating component is defined as $u'(\mathbf{x},t) = u(\mathbf{x},t) - \overline{u}(\mathbf{x})$, where $u(\mathbf{x},t)$ and $\overline{u}(\mathbf{x})$ are the total and mean values of the velocity, respectively, and $\mathbf{x} = (x,y,z)$ denotes the position vector. The coordinates $x$, $y$ and $z$ refer to the streamwise, spanwise and wall-normal directions, and the respective fluctuating velocity components are denoted by $u$, $v$ and $w$. Overbars indicate time-averaged values, and the superscript "+" is used to denote viscous scaling of length $z^+ = zU_\tau/\nu$ and velocities $u^+ = u/U_\tau$, where $\nu$ the kinematic viscosity of the fluid, $U_\tau = \sqrt{\tau_w/\rho}$ the friction velocity with $\tau_w$ the mean wall shear stress and $\rho$ the fluid density. The model is of the form:

$$u_p'^+(z^+,t^+) = u'^*(z^+,t^+)\left\{1+\chi(z^+)\,u_{OL}'^+(z_{OL}^+,t^+,\theta_L)\right\} + \alpha(z^+)\,u_{OL}'^+(z_O^+,t^+,\theta_L) \quad (1)$$

where $u_p'^+$ is the predicted time-series normalised by wall variables, $u_p'^+ = u_p'/U_\tau$ and $t^+ = tU_\tau^2/\nu$. The time-series $u'^*$, which is normalised in wall units, represents the statistically "universal" small-scale signal that would exist in the absence of any inner-outer interactions. $\alpha$ and $\chi$ are respectively the coefficients of superposition and modulation, whereas $\theta_L$ corresponds to the large-scale inclination angle to account for the streamwise shift between the two different wall-normal locations, $z^+$ and $z_O^+$ in equation 1. The model's parameters $u'^*$, $\alpha$, $\chi$ and $\theta_L$ are determined from a once-off calibration experiment at an arbitrarily chosen Reynolds number, and are hypothesized to be Reynolds number independent. The only user input required for the model is a characteristic signal of the large-scales from the log-region, $u_{OL}'^+$, taken nominally at the geometric centre of the log-layer, $z_O^+ = \sqrt{15Re_\tau}$, where $Re_\tau = U_\tau\delta/\nu$ is the friction Reynolds number, $\delta$ the boundary layer thickness (see Mathis *et al.*, 2009, 2011, for justifications about the choice of $z_O^+$). The model consists of two parts. The first part in equation 1 models the amplitude modulation of the small-scales, here $u'^*$, by the large-scale log-region motions, $u_{OL}'^+$. The second term, $\alpha u_{OL}'^+$, models the superposition of the large-scale motions felt at the wall. The underlying idea is that the near-wall small-scale motions are universal (i.e. they do not change with Reynolds number), and therefore only influenced by large-scale log-region events (the intensity of the influence increasing with increasing Reynolds number). Therefore, the Reynolds number effects are confined to the large-scale log-region input signal, $u_{OL}'^+$.

The purpose of the present study is to analyse the capabilities of this conceptual model to be extended to wall-bounded flows subjected to pressure gradient effects. In a previous study we have shown that the scale interaction mechanisms, superposition and modulation, remain similar in wall-bounded flows subjected to a pressure gradient effect, whether it is adverse (APG) or favourable (FPG) (Harun *et al.*, 2013). Spectral and scale decompositions show that the energy distributions are similar, with however some noticeable discrepancies. Importantly, the main differences between APG, ZPG and FPG flows are found to be in the large-scales associated with the log-region. In the APG case they are found to be more energetic compared to ZPG, whereas the opposite occurs for FPG flows. Meanwhile, the near-wall small-scale field appears to be relatively similar. These observations give us all confidence in possibility to extend the inner-outer predictive model to wall-bounded flows under pressure gradient effects. Besides, Adrian (2010) raised the question about the "truly" universality of the model's parameters ($u'^*$, $\alpha$, $\chi$ and $\theta_L$), *i.e.* are they or not dependent on the flow conditions, such as pressure gradient effects, roughness at the wall, etc? The present study also aims to shed some light on such an essential query.

## EXPERIMENTAL DATASET

In order to assess the behaviour of the model under pressure gradient effects and assess its universality, the model is calibrated independently in the different pressure gradient conditions. To do so, two separate calibration measurements have been performed, one in APG and one in FPG, whereas the ZPG calibration dataset comes from Mathis *et al.* (2011). Each measurement setup consist of two hot-wire probes separated in the wall-normal direction, sampled simultaneously in order to calibrate the predictive model for each pressure gradient condition. A fixed probe is located at the outer-spectral-peak location, $z_O^+ = \sqrt{15Re_\tau}$, as it has defined for ZPG condition (see Mathis *et al.* (2009)). It should be emphasised that we observed a slight change of this position under pressure gradient effects which tends to be closer to the wall as the FPG increases and away from the wall as the APG increases (see Harun *et al.* (2013)). Unfortunately, this has not been considered in the present calibration experiment, but an *a posteriori* test is given further within the paper to assess its effect. The fixed outer-probe is sampled simultaneously with a moving probe that traverses the inner region. Details of the main experimental conditions are given in Table 1. The friction velocity in APG and FPG configurations has been directly measured using oil-film interferometry (Chauhan *et al.*, 2010), whereas the Clauser chart is used in the ZPG case.

Table 1: Experimental conditions of the calibration measurements; $\beta = (\delta^*/\tau_w)(\mathrm{d}P/\mathrm{d}x)$ is the pressure gradient coefficient, where $\delta^*$ is the displacement thickness.

| | $Re_\tau$ | $\beta$ | $\nu/U_\tau$ | $l^+$ |
|---|---|---|---|---|
| APG | 3,300 | 1.55 | 31.7 | 15 |
| ZPG | 7,300 | 0 | 44.6 | 22 |
| FPG | 3,000 | -0.50 | 20.7 | 31 |

The corresponding turbulence properties, streamwise pre-multiplied energy spectra map and streamwise turbulence intensity are reported in Figure 1. In Figure 1$(d)$, the solid red symbol shows the location of the outer fixed probe, the open blue symbols the moving probe and open grey symbols results from a full traverse profile measurement. It should be emphasised that in order to avoid any bias in the streamwise Reynolds stress comparison, due to the disparity in the hot-wire sensor length $l^+$ (as see in Table 1), the spatial resolution correction method developed by Smits *et al.* (2011) is systematically applied.

Table 2: Overall flow conditions range of the database used for the validation test (from Harun (2012)).

| | $Re_\tau$ | $\beta$ | $l^+$ |
|---|---|---|---|
| APG | $1,750 : 3,900$ | $1.6 : 4.54$ | $15 : 31$ |
| FPG | $2,100 : 3,100$ | $-0.52 : -0.33$ | $17 : 31$ |

Once calibrated, the model's capabilities are assessed using a large database provided by the work of Harun (2012). These measurements consist of single hot-wire probe traverses, both in APG and FPG conditions, with variable Reynolds number and pressure gradient coefficient. Full details are available in Harun (2012). Table 2 summarises the overall range of flow conditions.

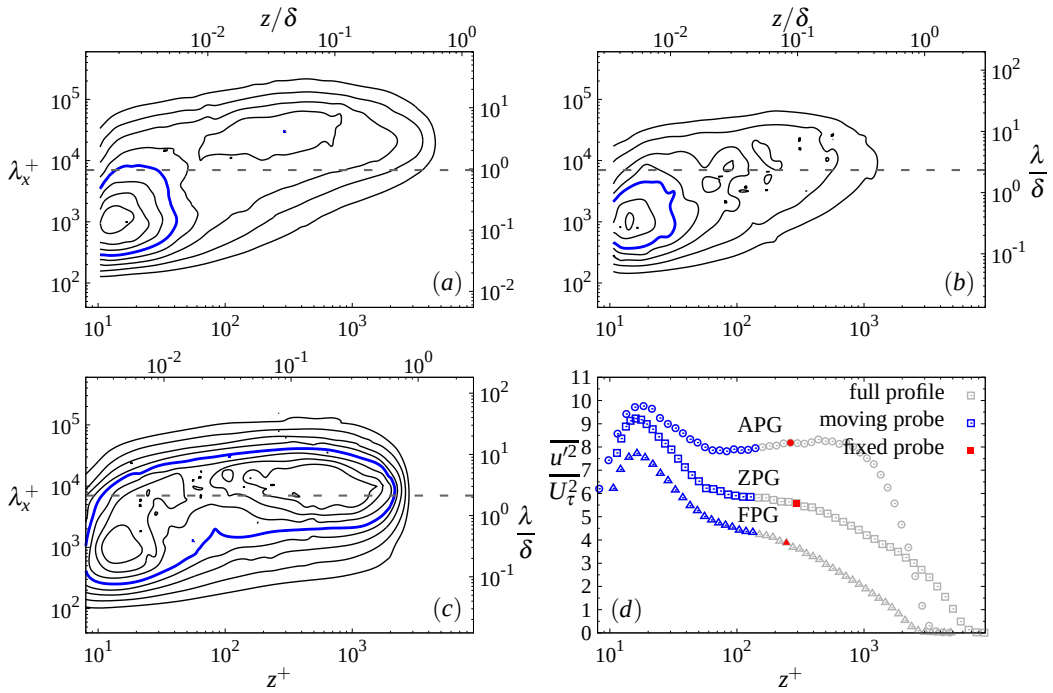


Figure 1: $(a-c)$ Streamwise pre-multiplied energy spectra map $k_x\phi_{uu}/U_\tau^2$. Contour levels are $0.2-1.6$ with 0.2 increments. The thicker blue contour corresponds to 0.1. $(d)$ Streamwise Reynolds stress profiles for all three cases (ZPG at $Re_\tau = 7300$, APG and ZPG at $Re_\tau \simeq 3000$).

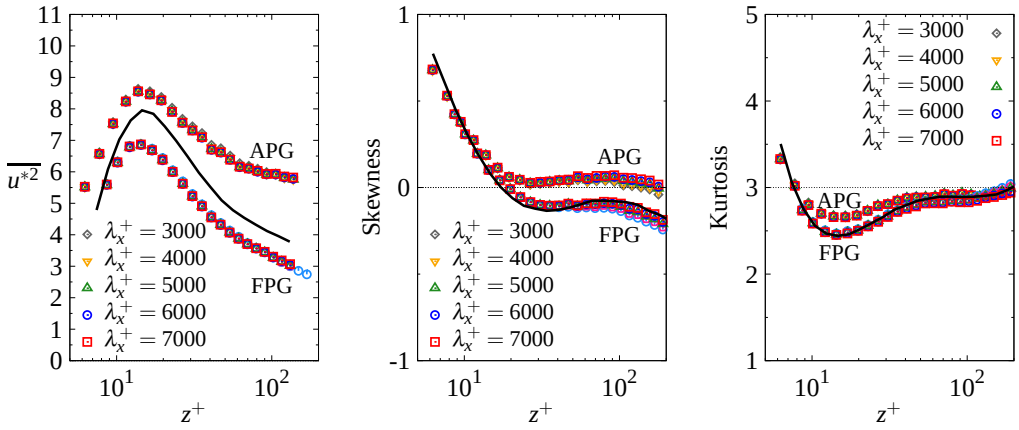


Figure 2: Universal signal's properties obtained for several cut-off wavelength; Solid black line corresponds to the universal signal properties from the ZPG model obtain with $\lambda_{x^+\,\mathrm{cutoff}} = 7000$.

## THE CALIBRATION

Details of the full calibration procedure are available in Mathis *et al.* (2011). Here, the goal is to apply it to the APG and FPG configurations, and to compare the universal parameters with the ones obtained in Mathis *et al.* (2011). However, before going through the calibration, it should be recalled that the procedure is based on scale decomposition, using a sharp filter in the Fourier space at a given cut-off wavelength. In the original procedure proposed by Mathis *et al.* (2011), the cut-off wavelength has been defined to $\lambda_x^+ = 7000$, as it was argued to be a good compromise to separate the inner- and outer-spectral peaks (see figure $1(a)$). This choice was shown to have no particular influence as long is in-between both peaks. However, under pressure gradient effects the cut-off wavelength choice becomes a little unclear. Indeed, as reported in Harun *et al.* (2013) FPG condition tends to attenuate the large-scale activity which induces a barely visible outer-peak in the spectral map (see figure $1(b)$). On the opposite, in APG condition the large-scale activity tends to be exacerbated which makes a wider outer-peak (in both wall-normal and wavelength directions on the spectra map, see figure $1(c)$). Therefore, a lower cut-off wavelength, say $\lambda_x^+ = 3000 \simeq \delta^+$, seems more appropriate. However, this raises the question of the real effect of the cut-off wavelength onto the parameters and accuracy of the model under pressure gradient effects. To avoid doubts, the calibration procedure is applied to the APG and FPG calibration datasets using a series of five cut-off wavelengths distributed between $\lambda_x^+ = 3000$ and 7000.

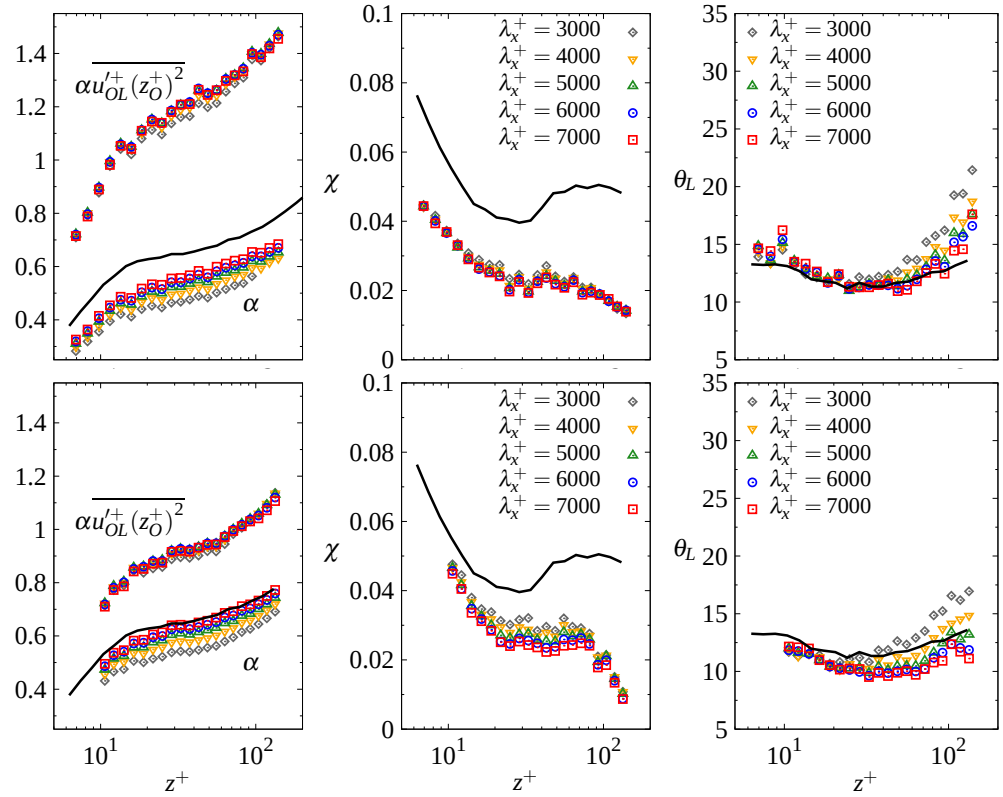


Figure 3: Model's parameters $\alpha$, $\chi$ and $\theta$ obtained for several cut-off wavelengths; Top: APG model; Bottom: FPG model; The product $\alpha\overline{u'^{+}_{OL}(z^{+}_{O})^{2}}$ is also depicted on left sub-figures; The solid black line corresponds to the universal signal properties from the ZPG model obtained using $\lambda_{x^+\,\mathrm{cutoff}} = 7000$.

The resulting statistics of the universal small-scale signal $u'^{*}$ and model's parameters, $\alpha$, $\chi$ and $\theta_L$, are given respectively in Figures 2 and 3, for both pressure gradient flows and compared to the ZPG model obtain using a cut-off wavelength $\lambda_{x^+\,\mathrm{cutoff}} = 7000$. At the first glance, the model's parameters seem not universal, in the sense that they are dependent on the flow configuration. This implies in the present state of the model that the calibration procedure needs to be done for each configuration. In future, the variability of flow condition would be more effective to be embedded within the model's parameters. However, this is beyond the scope of the present study, and constitutes a long-standing goal that requires substantial work and understanding about scales relationship in variable flow conditions, not only for pressure gradient, but for other effects such as roughness effect for instance. The aim of the present work, is to assess whether or not this model will lead us in the good direction.

However, some interesting features emerge. First, it is interesting to note that the universal small-scale signal $u'^{*}$ is independent of the chosen cut-off wavelength, for a given configuration. The only model's parameter affected by the chosen cut-off wavelength appears to be the superposition coefficient $\alpha$, which is directly link to the large-scales correlation coefficient (see Mathis *et al.* (2011). Indeed, the cut-off wavelength location changes directly the large-scales intensity, then their correlation. However, it is worth noting that the product, $\alpha\overline{u'^{+}_{OL}(z^{+}_{O})^{2}}$, remains constant as the cut-off wavelength is changing (see left hand side pictures in Figure 3), which explain why the universal small-scale signal is not affected. Indeed, the superposition term $\alpha\overline{u'^{+}_{OL}(z^{+}_{O})^{2}}$ in equation 1 is the main contributor to the energy, whereas the modulation term affects mainly the odd moments (see the discussion in Mathis *et al.*, 2011).

## MODEL ASSESSMENT

The model calibrated above for both APG and FPG flow conditions is tested on a wide database, provided by the work of Harun (2012), whose main characteristics are recalled in Table 2. This database allows us to evaluate the model's accuracy for varying Reynolds number and pressure gradient coefficient. Figures 4 and 5 show predicted statistics, respectively in APG and FPG boundary layer configuration. The left hand side of the figures is given for a fixed Reynolds number and varying pressure gradient coefficient, whereas in the right hand side pictures the pressure gradient coefficient is maintained constant and the Reynolds number is changing.

Overall, for both APG and FPG cases, the model seems to well capture the turbulence intensity, with both Reynolds number and pressure gradient effects captured. This is also visible on the predicted streamwise pre-multiplied energy spectra maps given in Figure 6. However, for higher moments the results are mitigated, as seen in Skewness and Kurtosis predictions. The reasons of the discrepancy remain unclear. One of the clue investigated was the location of the outer-spectral peak, as aforementioned discussed. Indeed, in previous work (Harun *et al.*, 2013), we observed that under pressure gradient condition, the outer-spectral peak

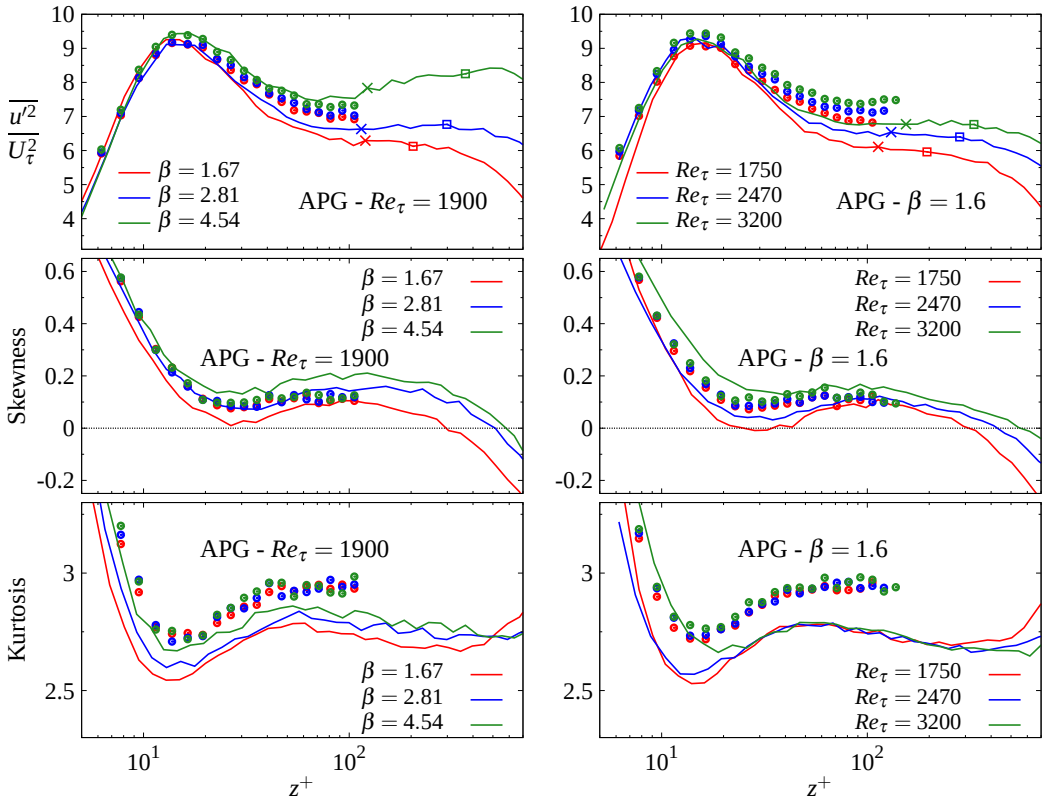


Figure 4: Comparison of the predictive statistics profiles (open symbols) against measurements (solid lines) for varying Reynolds number and pressure gradient coefficient in APG flows. In top sub-figures, the cross and open rectangle symbols depict respectively $z_O^+ = \sqrt{15Re_\tau}$ and $z_O^+|_{AM(z_O^+)=0}$.

location does not follow $z_O^+ = \sqrt{15Re_\tau}$ as in ZPG turbulent boundary layer. It was shown that the outer-peak location collapse with the location where the amplitude modulation coefficient crosses zero. Predictions made using $z_O^+$ such as $AM(z_O^+) = 0$ did not improve the results. The top sub-figures in Figure 4 and 5 depict the location of both $z_O^+ = \sqrt{15Re_\tau}$ (cross symbol) and $z_O^+|_{AM(z_O^+)=0}$ (open square symbol). Eventually, the effect of the cut-off wavelength discussed in the above section has also been investigated and no noticeable change was observed, this for all statistics up to the fourth order and spectra maps.

## DISCUSSION AND CONCLUSION

The present work is devoted to the extension of the inner-outer predictive model of Marusic *et al.* (2010) to wall-bounded flows subjected to pressure gradient effects. Preliminary findings presented here show encouraging results, as well highlight the need of further work to generalise such a model. The model is able to predict the energy content, *i.e.* the streamwise turbulence intensity and spectra, but lacks to predict higher order statistics. Moreover, it turns out that the model's calibration needs to be redone when external conditions change (*i.e.* APG, FPG, ...), emphasising the non-universality of the parameters. Finally, it should be mentioned that the range of Reynolds number presented here remains limited to fully test and eventually understand scales interaction subjected to pressure gradient. This draws the need, as previously occured in ZPG studies, for high Reynolds number dataset, at least one order of magnitude than the ones presented here. However, if some ZPG facilities exist, capable of producing such results, no facility can yet provide similar high Reynolds number measurements under pressure gradient effects, at least one that can afford to be spatially and temporally resolved (Hutchins *et al.*, 2009).

## REFERENCES


Adrian, R. J. 2007 Hairpin vortex organization in wall turbulence. *Phys. Fluids* **19**, 041301.

Adrian, R. J. 2010 Closing in on models of wall turbulence. *Science* **329** ((5988)), 155–156.

Adrian, R. J., Meinhart, C. D. & Tomkins, C. D. 2000 Vortex organization in the outer region of the tubulent boundary layer. *J. Fluid Mech.* **422**, 1–54.

Cantwell, B. J. 1981 Organized motion in turbulent flow. *Annu. Rev. of Fluid Mech.* **13**, 457–515.

Chauhan, K. A., Ng, H. C. H. & Marusic, I. 2010 Empirical mode decomposition and Hilbert transforms for analysis of oil-film interferograms. *Meas. Sci. Tech.* **21** (105404), 1–13.

Dennis, D.J.C. & Nickels, T.B. 2011 Experimental measurement of large-scale three-dimensional structures in a turbulent boundary layer. part 2. long structures. *J. Fluid Mech.* **673**, 218–244.

Harun, Z. 2012 The structure of adverse and favourable pressure gradient turbulent boundary layers. PhD thesis, The University of Melbourne.

Harun, Z., Monty, J. P., Mathis, R. & Marusic, I. 2013 Pressure gradient effects on the large-scale structure of turbulent boundary layers. *J. Fluid Mech.* **715**, 477–498.

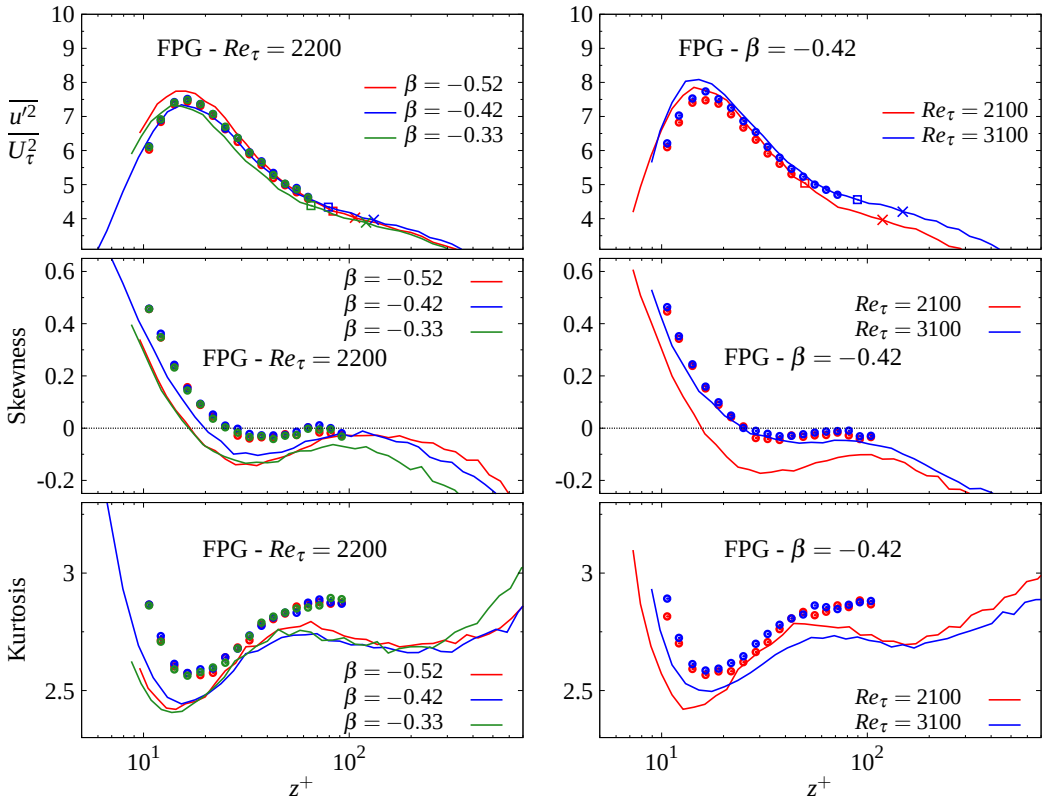


Figure 5: Comparison of the predictive statistics profiles (open symbols) against measurements (solid lines) for varying Reynolds number and pressure gradient coefficient in FPG flows. In top sub-figures, the cross and open rectangle symbols depict respectively $z_O^+ = \sqrt{15 Re_\tau}$ and $z_O^+|_{AM(z_O^+)=0}$.

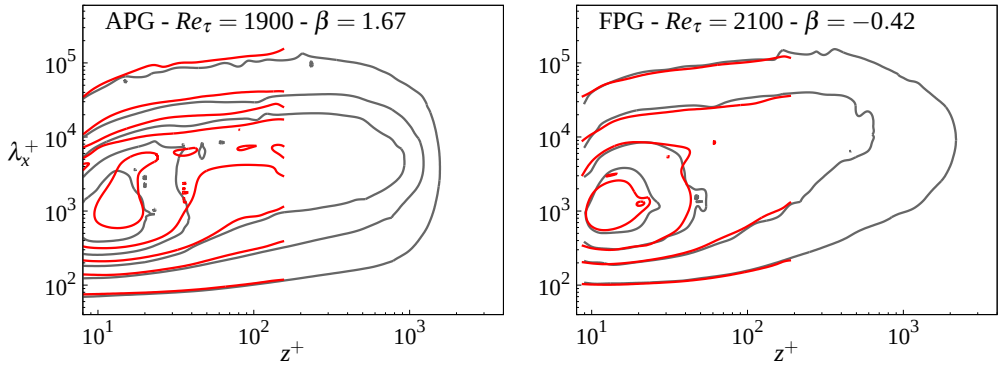


Figure 6: Examples of reconstructed streamwise pre-multiplied energy spectra maps $k_x\phi_{uu}/U_\tau^2$ (red contours) against measurements (grey contours) for APG and FPG flows. Contour levels are $0.2 - 1.6$ with 0.4 increments.


Hutchins, N. & Marusic, I. 2007 Evidence of very long meandering features in the logarithmic region of turbulent boundary layers. *J. Fluid Mech.* **579**, 1–28.

Hutchins, N., Nickels, T., Marusic, I. & Chong, M. S. 2009 Spatial resolution issues in hot-wire anemometry. *J. Fluid Mech.* **635**, 103–136.

Kim, K. C. & Adrian, R. J. 1999 Very large-scale motion in the outer layer. *Phys. Fluids* **11**, 417–422.

Marusic, I., Mathis, R. & Hutchins, N. 2010 Predictive model for wall-bounded turbulent flow. *Science* **329** (5988), 193–196.

Mathis, R., Hutchins, N. & Marusic, I. 2009 Large-scale amplitude modulation of the small-scale structures in turbulent boundary layers. *J. Fluid Mech.* **628**, 311–337.

Mathis, R., Hutchins, N. & Marusic, I. 2011 A predictive inner-outer model for streamwise turbulence statistics in wall-bounded flows. *J. Fluid Mech.* **681**, 537–566.

Smits, A. J., Monty, J. P., Hultmark, M., Bailey, S. C. C., Hutchins, N. & Marusic, I. 2011 Spatial resolution correction for wall-bounded turbulence measurements. *J. Fluid Mech.* **676**, 41–53.

Townsend, A. A. 1976 *The Structure of Turbulent Shear Flow*, 2nd edn. Cambridge: Cambridge University Press.